Effect of Ionic Chain Polydispersity on the Size of Spherical Ionic Microdomains in Diblock Ionomers

Diep Nguyen,[†] Xing-Fu Zhong,[†] Claudine E. Williams,*[,‡] and Adi Eisenberg*[,†]

Department of Chemistry, McGill University, Montreal, Quebec, Canada H3A 2K6, and Laboratoire pour l'Utilisation du Rayonnement Électromagnétique (LURE), CNRS-CEA-MEN, Université Paris-Sud, 91405 Orsay Cedex, France

Received February 2, 1994; Revised Manuscript Received May 19, 1994[®]

ABSTRACT: The effect of ionic chain polydispersity on the morphology of spherical ionic microdomains in the dry state is studied by small-angle X-ray scattering (SAXS) and transmission electron microscopy (TEM) for two systems of diblock ionomers, polystyrene-*b*-poly(4-vinylpyridinium methyl iodide) (PS-*b*-P4VPMeI) and polystyrene-*b*-poly(cesium methacrylate) (PS-*b*-PMACs). The polydispersity of the ionic blocks is controlled by blending diblock copolymers of constant polystyrene length but different ionic block lengths. The samples are mixed in appropriate ratios so that the number-average molecular weight is constant but a wide range of polydispersity in the ionic blocks is obtained. The samples are prepared by three different methods. The first method involves preparation from a solution in which a nonequilibrium state exists. This is carried out either by addition of a nonsolvent to the single-chain polymer solution (as for the PS-*b*-P4VPMeI series in DMF) or by neutralization in a selective solvent (as for the methacrylic acid copolymers in THF). In the second method, the PS-*b*-P4VPMeI samples are cast from a good solvent for both blocks. Finally, in the third method, the 4-vinylpyridine diblocks are mixed before quaternization and then cast from THF. Electron micrographs show a regular arrangement of spherical ionic microdomains and ruled out dual morphology. The radii of the ionic microdomains of samples prepared by methods 2 and 3 are found to increase linearly with the ionic chain polydispersity, while those which are prepared by method 1 stay constant. This difference is explained in terms of the thermodynamic conditions prevailing in the solutions at the onset of microphase separation.

Introduction

The bulk morphology of ionic AB di- and ABA triblock copolymers has raised much interest lately.[1-10] The strong incompatibility between the ionic and nonionic moieties results in the formation of microphases where the local physical properties (e.g., dielectric constant, solvation, etc.) are very different. The various morphologies observed are similar to those of their nonionic counterparts; when the nonionic blocks are long and the ionic ones are relatively short, the ionic domains are spherical and dispersed in a nonionic continuous phase. They act as strong ionic cross-links, which gives the material very specific mechanical properties. A broadening of the rubbery plateau and an increase in the modulus and tensile strength are among the observed effects.[3,7] These polymers qualify as a special class of ionomers, the block ionomers, as opposed to the random ionomers where the ionic units are randomly distributed along the long nonionic polymer. In these materials, the ion pairs tend to aggregate in media of low dielectric constant, and the presence of these ionic aggregates modifies the properties of the polymer profoundly.[10]

The first experimental study of the structure of block ionomers by small-angle X-ray scattering (SAXS) dealt with ABA triblock copolymers with a long nonionic midblock of polystyrene (PS) and relatively short ionic end blocks of poly(4-vinylpyridinium methyl iodide).[4] In that study, it was shown that the ionic blocks, even at very short ionic block lengths, associated into spherical microdomains organized on a highly distorted cubic lattice. The size of the ionic microdomains was found to be independent of the PS block length and the ionic blocks were highly extended. In contrast, the PS chains had a coiled configuration, as shown by small-angle neutron scattering (SANS).[5] High extension of the ionic sequences in their microdomains was also reported by Venkateshwaran *et al.*[6] for the methacrylate-based AB and ABA block ionomers. More systematic SAXS experiments on AB and ABA block ionomers[8] of short ionic block lengths of polystyrene-*b*-poly(vinylpyridinium methyl iodide) or polystyrene-*b*-poly(cesium methacrylate) have confirmed that the radii are of the same order as the stretched length of the ionic blocks independent of architecture (AB or ABA), chemical structure (4-vinylpyridinium methyl iodide or cesium methacrylate), or method of preparation (casting or molding). The high extension of the ionic chains has been discussed theoretically by Doi *et al.*[11] when investigating phase separation of block copolymers in a superstrong (very large χ) segregation regime.

One puzzling finding of these investigations is the fact that, in some cases, the radii of the microdomains are larger than the fully extended chain length. One way of explaining this fact is to invoke a molecular weight distribution. Given a molecular weight distribution, it is possible to envisage the longest chains extending all the way to the center of the microdomains, with the shorter chains occupying the regions closer to the surface. Consequently, the longest chains would play an important role in determining the radius. Since the studies discussed above used mostly block copolymers of low polydispersity (1.1–1.2), only a mild enlargement of the ionic radius with respect to the ideal monodisperse case is seen.

To check the validity of this hypothesis, samples have been prepared with a controlled and increasing polydispersity of the ionic block lengths by mixing different copolymers with constant PS lengths and various nominal ionic block lengths in such a way that the average molecular weights of the sample stay constant; thus, samples with a wide range of molecular weight distributions are generated. Because reaching thermodynamic equilibrium may be a problem in these highly incompatible systems,

---

[*] To whom correspondence should be addressed.

[†] McGill University.

[‡] LURE, CNRS-CEA-MEN, Université Paris-Sud.

[®] Abstract published in *Advance ACS Abstracts,* July 15, 1994.

0024-9297/94/2227-5173$04.50/0 © 1994 American Chemical Society

different methods of sample preparation have been used. Reports of studies which dealt with the molecular weight distribution effect in block copolymers have appeared before.[12,13] However, this paper is the first that reports the results of a morphological investigation of diblock ionomers with a broad range of molecular weight distributions prepared by mixing different diblock ionomers of different chain lengths. The experimental methods employed are X-ray scattering and transmission electron microscopy. It will be shown that polydispersity may have an influence on the size of the ionic microdomains but that the strength of the effect is very much affected by the methods of sample preparation.

Experimental Section

1. **Materials and Sample Preparation.** The polystyrene-*b*-poly(methacrylic acid) copolymers were synthesized in connection with another project.[7] The syntheses of diblock copolymers of polystyrene-*b*-poly(4-vinylpyridine) (PS-*b*-P4VP) and polystyrene-*b*-poly(methacrylic acid) (PS-*b*-PMA) were carried out following known procedures;[14-16] thus, only a brief summary is given here. The AB diblock copolymers were synthesized by sequential anionic copolymerization of styrene monomer followed by *tert*-butyl methacrylate or 4-vinylpyridine monomer, using *n*-butyllithium as the initiator. The polymerization was performed in tetrahydrofuran (THF) at 78 °C under a nitrogen atmosphere. The apparatus used for the polymerization allowed the withdrawal of reaction mixture in the course of the synthesis. Thus, for a given constant polystyrene block length, a series of diblocks was obtained with poly(*tert*-butyl methacrylate) or poly(4-vinylpyridine) segments of lengths varying from ca. 10 to 100 units. Aliquots of the reaction mixtures were also withdrawn for characterization after the polystyrene block was formed and every time after the second monomer was added.

Polystyrene-*b*-poly(methacrylic acid) copolymers were obtained by acid-catalyzed hydrolysis of the *tert*-butyl methacrylate segments in toluene at 80 °C using *p*-toluenesulfonic acid (PTSA) as the catalyst.[14] The PS-*b*-PMA was recovered and purified by repeated precipitation in methanol, methanol/water mixtures, or water depending on the composition of the diblocks. The PS-*b*-P4VP was recovered and purified by repeated precipitation in hexanes.

The acid contents of the PS-*b*-PMAA copolymers were determined in THF/H_2O mixtures using aqueous NaOH as titrant and phenolphthalein as the indicator. The 4-vinylpyridine content of the PS-*b*-P4VP series was determined by nonaqueous titration of the vinylpyridine segments with perchloric acid.

For the quaternization of the poly(4-vinylpyridine) blocks, the polystyrene-*b*-poly(4-vinylpyridine) copolymers were dissolved in dried THF (5% solution), and freshly distilled methyl iodide was added in 10-fold excess. The reaction solution was refluxed under nitrogen for 3–4 h to achieve full quaternization. The disappearance of the 1414 cm^{-1} 4VP IR band was taken as evidence of complete quanternization.[16] The copolymers were recovered by precipitation in 2-propanol (10-fold volume excess) and were dried in a vacuum oven at 60 °C.

The molecular weight of the polystyrene block was determined, with a precision of ±5%, by size exclusion chromatography (SEC) in THF using narrow molecular weight polystyrene standards. The polydispersity indexes or the molecular weight distributions of the PS blocks were around 1.10 and those of the diblocks (poly(*tert*-butyl methacrylate) precursor in the case of the methacrylate diblocks) were found to vary from 1.1 to 1.3.

Two series of samples were prepared. It is important to note that in each series the molecular weights as well as the molecular weight distributions of the PS blocks were kept constant; only those of the diblock copolymers were changed. The first consisted of a polystyrene block of molecular weight of 170 units (17.3×10^3 g/mol) and poly(methacrylic acid) blocks ranging from 9 to 100 units (8×10^2 to 8.8×10^3 g/mol); the second was a series with a polystyrene of molecular weight of 470 units (49.0×10^3 g/mol) and poly(4-vinylpyridine) blocks ranging from 7 to 95 units (7×10^2 to 9.8×10^2 g/mol).

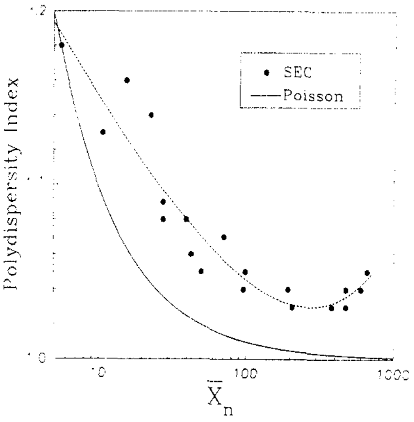

Figure 1. Theoretical and experimental values of chain polydispersity index as a function of molecular weights of homopolymers. The solid line is the calculated Poisson distribution curve; the dashed line is a guide for the eye which is fitted through the experimental points by the least squares method.

The abbreviations used to indicate the copolymer compositions are as follows: PS(470)-*b*-P4VP(25) means a polystyrene chain of 470 units joined to a poly(4-vinylpyridine) chain of 25 units. The quaternized form will be denoted by the suffix MeI. Similarly, PS(170)-*b*-PMACs(25) indicates a polystyrene chain of 170 units joined to a poly(methacrylic acid) chain of 25 units neutralized with CsOH.

2. **Sample Preparation for SAXS.** It is worth recalling here that the polydispersity index, PI, is defined as the ratio of the weight-average molecular weight, M_w, to the number-average molecular weight, M_n. $M_w = \sum N_iM_i^2/\sum N_iM_i$ and $M_n = \sum N_iM_i/\sum N_i$, where N_i and M_i are the numbers of moles and molecular weights of the individual blocks. Samples of controlled polydispersities were prepared by mixing diblock copolymers of the same PS length but with different ionic block lengths in various molar ratios. This was done to ensure that, in a set of samples, the number-average molecular weight of the blends, i.e., the average number of units in the ionic blocks, stays constant but that the ionic chain polydispersity index (ICPI) increases.

The determination of the ICPI involved two steps. In the first one, the polydispersity of the ionic block in the diblock is determined; then, the ICPI of the blends is calculated.

It is not possible to determine the polydispersity of the ionic blocks, i.e., the second block in the diblock, by conventional experimental techniques, e.g., SEC. In principle, one should be able to calculate the polydispersity of the second block if the polydispersity of the first block and the total distribution are known.[17,18] However, in the present case, the molecular weight difference between the PS block and the diblock is too small for such a method and, therefore, the ICPIs were estimated by the following method. It is based on the assumption that the molecular weight distributions of the second blocks (4VP or MAA) in the diblock chains are the same as those of homopolymers of polystyrene of comparable lengths. Therefore, a number of short homopolymers of polystyrene were prepared by the anionic polymerization technique, and their polydispersities were measured by SEC; a Poisson distribution function was also calculated since it is supposed to describe the molecular weight distribution of polymers obtained by anionic polymerization.[19] The results are presented in Figure 1. It appears that the experimental distributions are generally broader than predicted by the Poisson distribution. Thus, the molecular weight distributions of the poly(4-vinylpyridine) or poly(methacrylic acid) blocks were estimated from the experimental curve in Figure 1.

The calculation of ICPIs of the blends was carried out as follows: since the Poisson distribution is clearly not applicable, a Gaussian distribution in the molecular weight is assumed, which is given mathematically by the function[19]

$$f(x) = \frac{1}{(\sigma_n)(2\pi)^{1/2}} \exp\left[-\frac{(x - x_n)^2}{2\sigma_n^2}\right] \qquad (1)$$

where $\sigma_n = x_n(\mathrm{PI} - 1)^{1/2}$, x_n is the average degree of polymerization,

Table 1. Composition of Blends and Their ICPIs

detailed composition of the blends[b]	ICPI
PS(470)-*b*-P4VPMeI(17)[a]	
(17) × 1	1.14
(36) × 2 + (17) × 2 + (7) × 4	1.6
(52) × 1 + (26) × 1 + (7) × 4	2.1
(71) × 1 + (36) × 1 + (7) × 7	2.6
(94) × 1 + (36) × 1 + (7) × 9	3.3
(94) × 1 + (7) × 6	3.6
Binary Blends of PS(470)-*b*-P4VPMeI(26)[a]	
(26) × 1	1.11
(52) × 1 + (17) × 3	1.5
(71) × 2 + (17) × 10	1.7
(94) × 1 + (17) × 7	2.0
PS(170)-*b*-PMACs(25)[a]	
(25) × 1	1.11
(50) × 4 + (25) × 3 + (9) × 6	1.6
(100) × 1 + (25) × 6 + (9) × 5	2.1
(100) × 1 + (25) × 2 + (9) × 5	2.6
(100) × 1 + (9) × 5	3.1

[a] Within each series, the number-average molecular weight of the ionic blocks is kept constant. [b] The number in parentheses indicates the number of units of ionic blocks, and the number outside the parentheses is the number of parts (by moles) of the corresponding diblock in the blends. The length of the PS block is kept constant

and PI is the polydispersity index of the polymer. In the calculation, symbols for the ICPI and the number of units in the ionic block were taken as PI and x_n, respectively. For each component in the blend, the molecular weight distribution curve, $f_i(x)$, was constructed from the average degree of polymerization and polydispersity. The molecular weight distribution curve of the blend, $f(x)$, was then calculated by taking the summation of all the $f_i(x)$ and in proportion to their ratio of mixing and their polydispersity. The M_w and M_n of the blends were deduced from the function $f(x)$, and their ratio gave the required ICPIs.

As an example, the preparation of a diblock of PS(470)-*b*-P4VPMeI(17) with an ICPI of 1.6 from the series of different ionic block lengths of low polydispersity is given here. Four parts (by moles) of PS(470)-*b*-P4VP(7) with an ICPI of 1.18 were mixed with two parts (by moles) of PS(470)-*b*-P4VP(35) with an ICPI of 1.08 and two parts (by moles) of PS(470)-*b*-P4VP(17) with an ICPI of 1.14. The resulting blend had the same M_n as the "parent" PS(470)-*b*-P4VP(17) copolymer; however, the blend sample had an ICPI equal to 1.6.

For all the systems, blends contain more than two different chain lengths and are referred to as multicomponent blends. In addition, for the PS-*b*-P4VPMeI copolymers, binary mixtures in which there are only two different chain lengths were also prepared. The detailed blend compositions and the ICPI values are listed in Table 1.

The PS-*b*-PMAA diblocks were mixed in the acid form in dry THF (3 wt %). The acid solutions were neutralized by the dropwise addition of stoichiometric amounts of methanolic CsOH. The solutions were stirred for 2–3 h and the solvents were allowed to evaporate under ambient conditions to produce thin and brittle films.

Thin films of the PS-*b*-P4VPMeI blends were prepared by three different methods. In method 1 (M1), the calculated molar ratios of the vinylpyridinium methyl iodide blocks were dissolved and mixed in dimethylformamide (DMF) to produce 5% (w/w) solutions. Toluene, a nonsolvent for the ionic segments, was added dropwise to the solutions. Upon addition of toluene, the diblock copolymers formed micelles which consisted of a core of the P4VPMeI blocks and a corona of PS segments. The polymers were recovered by precipitation into excess 2-propanol (5 times the volume of the polymer solution). The resulting blends were redissolved and cast from toluene. In method 2 (M2), the PS-*b*-P4VPMeI polymers were mixed in the appropriate molar ratios in DMF (5 wt %). The solutions were allowed to evaporate under a reduced pressure of 0.5 atm at room temperature. In method 3 (M3), the PS-*b*-P4VP copolymers were mixed in THF, followed by the quaternization process. The solutions were subsequently allowed to evaporate under ambient conditions.

Thin films of the unmixed copolymers were also prepared by the same methods as those described above for the blends in both systems of diblocks, except for the PS-*b*-P4VPMeI series in which methods 1 and 2 only were employed.

All films were vacuum dried at 110 °C for 3 days. They were stored in a desiccator until used for the SAXS measurements.

3. SAXS Instrumentation. The small-angle X-ray scattering experiments were performed at the D22 station of the LURE–DCI synchrotron radiation source (Orsay, France). A description of the spectrometer has been published elsewhere.[20,21] It is a specialized spectrometer equipped with a double-crystal, fixed-exit monochromator providing a beam of a narrow energy range tunable from 4 to 15 keV (3–0.8 Å). The size of the beam at the sample was about 1 mm^2. The experiments were done under vacuum. The scattered X-rays were detected with a Xe–CO$_2$ gas filled, one-dimensional position-sensitive detector with a resolution of 152 μm. All samples were studied in the angular q range from 0.006 to 0.30 Å^{-1} ($q = 4\pi \sin \Theta/\lambda$, where Θ is half the scattering angle and λ is the X-ray wavelength). The resulting intensity, I, vs q curves were corrected for beam decay, sample absorption, and sample thickness; background scattering from a polystyrene homopolymer or from the empty sample holder was subtracted. The q resolution was of the order of 0.003 Å^{-1}.

4. Transmission Electron Microscopy. Transmission electron microscopy (TEM) observations were made with a Philips EM410-LF electron microscope operated at 80 kV. Thin sections of samples of about 600 Å thickness were obtained by microtoming the diblock ionomer films at room temperature. The samples were cut both perpendicular and parallel to the film surface and were stained with osmium tetraoxide (OsO$_4$).

Results and Discussion

The Results and Discussion is divided into five parts. Transmission electron micrographs are discussed in part 1. SAXS profiles along with descriptions of the data treatment are presented in part 2. The fitting of the shape factor peaks and the results for the values of the radii are presented in parts 3 and 4, respectively. Finally, part 5 contains a discussion of the values of the aggregation number (N) and the surface area per chain (S/N).

1. Transmission Electron Microscopy Results. Figures 2 and 3 show transmission electron micrographs for samples prepared by method 2 of the multicomponent blend of PS(470)-*b*-P4VPMeI(17) of ICPI of 1.6 and of the binary blend of PS(470)-*b*-P4VPMeI(26) of ICPI of 2.0. The dark domains are the P4VPMeI blocks and the bright regions are the unstained PS segments. Due to the microtoming process, some stretching of the samples occurred; therefore, no attempt was made to determine the size of the microdomains from the TEM results, and only qualitative information about the shape was extracted. From the micrographs, it can be seen that the P4VPMeI blocks organize in spherical domains and that there is no dual morphology.

2. Data Treatment and SAXS Profiles. The intensity $I(q)$ scattered by an isotropic assembly of interacting particles can be expressed as the *product* of the shape factor, $P(q)$, which describes the size and shape of a single particle, times the structure factor, $S(q)$, which characterizes the spatial correlation between the particles.[22] A structural description of the system requires obtaining each function separately. In most cases, this cannot be achieved directly from a single scattering measurement, and one has to use more sophisticated techniques (contrast variation, dilution, etc.) or model fitting.[22] One exception is when the size of the particles is much smaller than the characteristic distances between them and thus, the features associated with $P(q)$ and $S(q)$ appear in different regions of the scattering profiles. Previous investigations of the same family of materials have shown that such is the case for most of these block ionomers, especially in

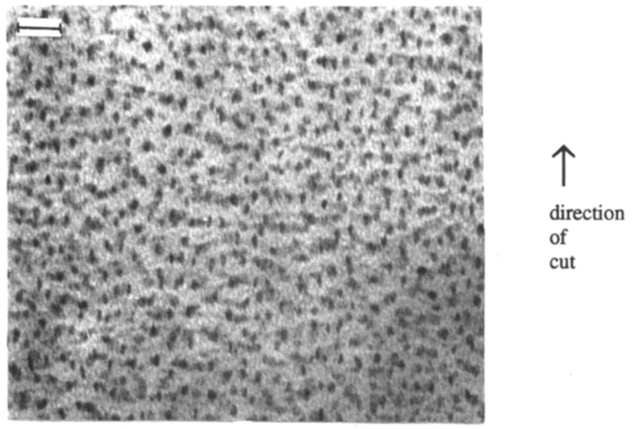

a) Section cut perpendicular to the surface of the film.

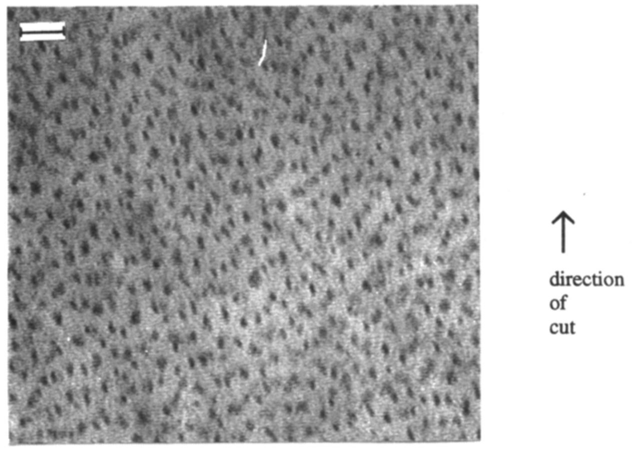

b) Section cut parallel to the surface of the film.

Figure 2. Transmission electron micrographs of sections, 600 Å thick, of a sample of PS(470)-*b*-P4VPMeI(17), a multicomponent blend of an ICPI of 1.6; (a) and (b) are sections cut perpendicular and parallel to the surface of the film, respectively. The bar indicates a length of 275 Å.

solution.[8,24] Indeed, the structure peaks appear at low q, and the shape factor peak extends at higher angles where $S(q)$ has reached its asymptotic value of 1.

Since the relative volume fractions of the ionic blocks in this study are low,[23] 5% in the P4VPMeI and 13% in the PMACs, the ionic segments self-assemble into spherical microdomains. This is also confirmed by the TEM micrographs even for high ICPI, as seen in Figures 2 and 3. The shape factor of a sphere of radius R can be calculated analytically as[22]

$$P(q) = \left[3\frac{\sin(qR) - qR\cos(qR)}{(qR)^3}\right]^2 \qquad (2)$$

Equation 2 has its zeros at $qR = 4.5, 7.7$, etc. and its maxima at $qR = 5.8, 9.1$, etc. The position of the zeros gives directly a measurement of the radius. Polydispersity in particle sizes smears out the features and the zeros transform into shallow minima. The first minimum can be seen in the region from 0.08 to 0.1 Å in the scattering profiles of the samples with low ICPI in Figures 4–6, and two minima are seen in Figure 7. In some samples, the shape factor features are washed out completely.

An estimate of the radius can also be obtained using the structure factor peak. From the positions of the structure peaks, one can estimate the Bragg spacings, d_B, using the Bragg equation. Knowing the Bragg distance and the volume fraction of each component, it is possible, by using simple crystallographic, geometric, and space-filling arguments, to compute the radius of spheres arranged on different types of lattices: simple cubic (sc), body centered cubic (bcc), face centered cubic (fcc), and hexagonal close packed (hcp). for this calculation, it is assumed that the materials are completely phase separated and that a negligible interphase thickness is involved. This assumption is reasonable taking into account the high driving force for phase separation between ionic and nonionic segments[4,8] and the asymptotic variation of intensity as q^{-4}. The relative structure peak positions are expected to be at certain q values for a particular lattice; for example, in the case of the simple cubic lattice, the relative angular positions of the peaks are 1, $\sqrt{2}$, $\sqrt{3}$, 2, etc. In the absence of more than one well-defined structure peak, it is impossible to ascertain the type of lattice that the system belongs to.

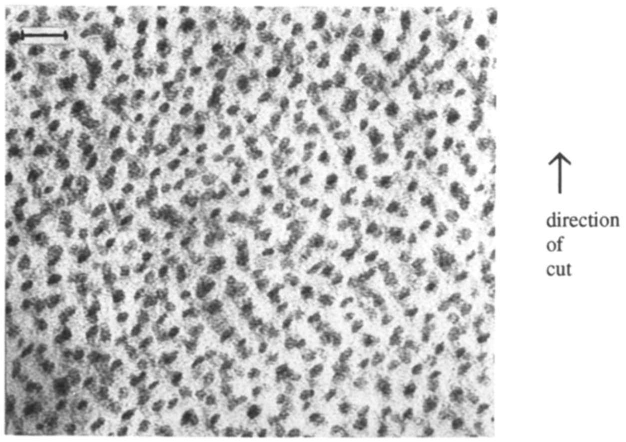

a) Section cut perpendicular to the surface of the film.

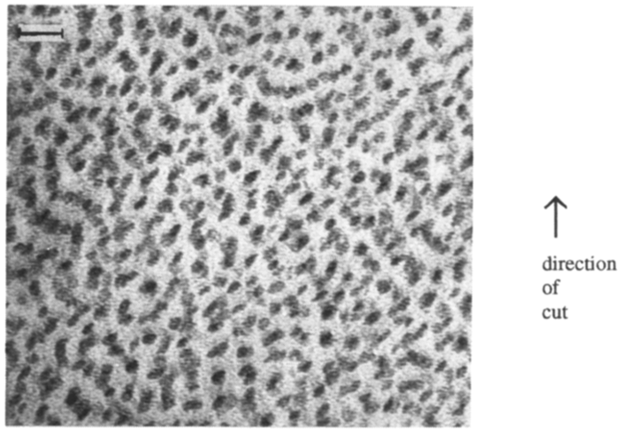

b) Section cut parallel to the surface of the film.

Figure 3. Transmission electron micrographs of sections, 600 Å thick, of a sample of PS(470)-*b*-P4VPMeI(26), a binary blend of an ICPI of 2.0; (a) and (b) are sections cut perpendicular and parallel to the surface of the film, respectively. The bar indicates a length of 275 Å.

Since the shape factor features give a direct measurement of the radii, these values are deemed more reliable than those calculated based on space-filling arguments. However, the shape factor features are not observed in all samples due to sample polydispersity, as explained in section 3 below. In that case, from the comparison between the radius obtained from the shape factor peaks, when available, and those from the first maximum using space-filling calculations, one can determine the lattice that gives the least difference between the two sets of values. The radii obtained from space-filling calculations assuming this lattice are reported. It should be stressed that the

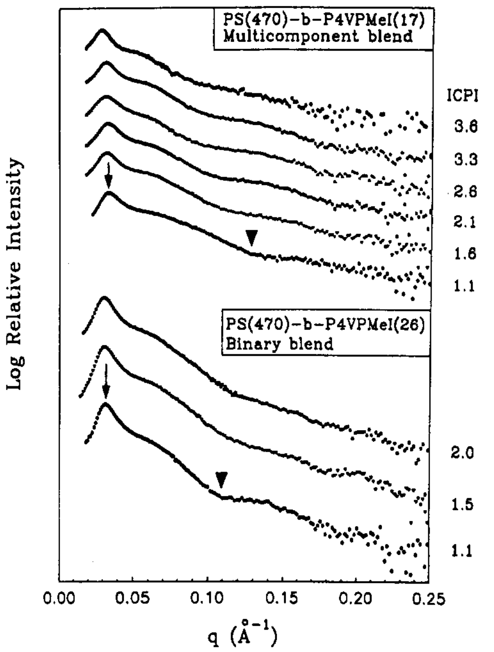

Figure 4. SAXS profiles of multicomponent blends of PS(470)-*b*-P4VPMeI(17) and of binary blends of PS(470)-*b*-P4VPMeI(26) prepared by method 1. In two of the SAXS profiles the minima of the shape factor are marked by a dark triangle and the structure peaks are marked by a single arrow. Successive profiles have been shifted vertically for clarity.

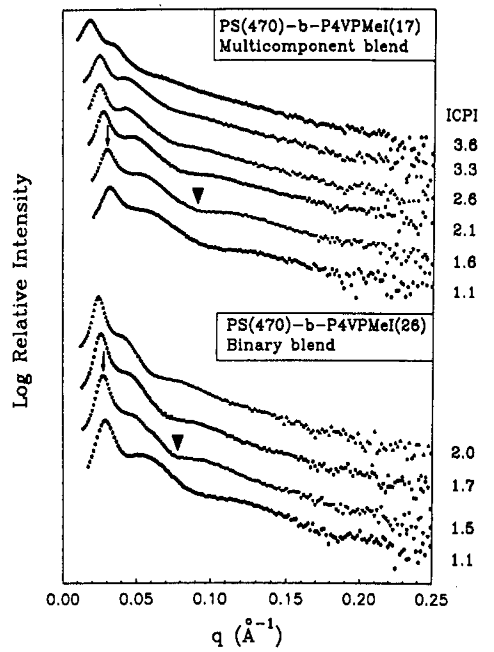

Figure 5. SAXS profiles of multicomponent blends of PS(470)-*b*-P4VPMeI(17) and of binary blends of PS(470)-*b*-P4VPMeI(26) prepared by method 2. In two of the SAXS profiles the minima of the shape factor are marked by a dark triangle and the structure peaks are marked by a single arrow. Successive profiles have been shifted vertically for clarity.

use of a particular lattice in the calculation does not necessarily imply that a macrocrystal arrangement of spherical microdomains is observed. It is even possible that the real structure resembles that of an amorphous material. In the experimental SAXS profiles (Figures 4–7) the minima of the shape factor are marked by a dark triangle and the structure peaks are marked by a single arrow.

Figure 4 shows the SAXS intensity profiles for the PS-*b*-P4VPMeI samples, for both the multicomponent and binary blends, prepared by method 1. A broad peak with a pronounced shoulder is observed. The shape factor peaks are seen for multicomponent mixtures of an ICPI up to 3.0, while for the binary mixtures, the shape factor peaks become so weak that the scattered intensities diminish considerably. Figure 5 shows the SAXS intensity profiles for the PS-*b*-P4VPMeI samples, for both the multicomponent and binary blends, prepared by method 2. A broad, asymmetric peak along with a well-defined secondary shoulder is seen. The shape factor peaks are seen for all

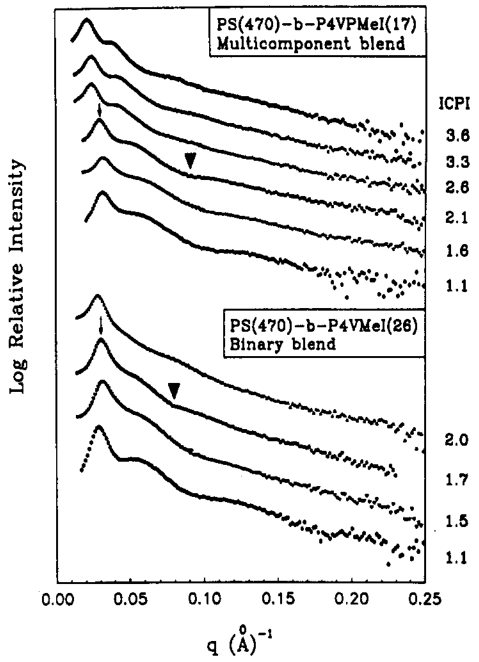

Figure 6. SAXS profiles of multicomponent blends of PS(470)-*b*-P4VPMeI(17) and of binary blends of PS(470)-*b*-P4VPMeI(26) prepared by method 3. In two of the SAXS profiles the minima of the shape factor are marked by a dark triangle and the structure peaks are marked by a single arrow. Successive profiles have been shifted vertically for clarity.

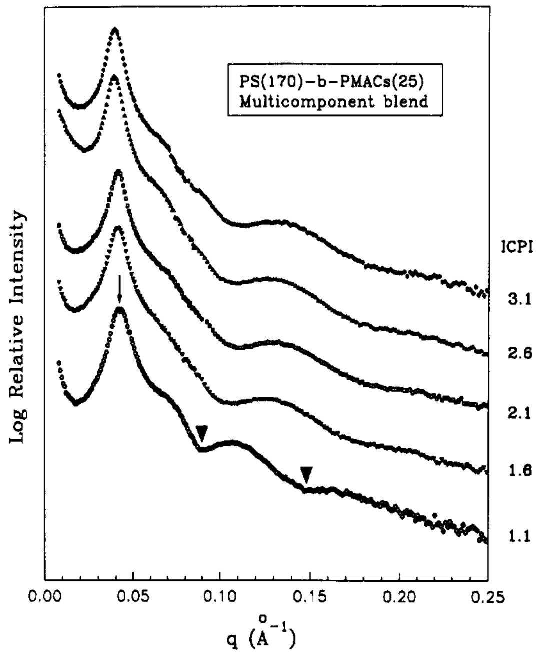

Figure 7. SAXS profiles of multicomponent blends of PS(170)-*b*-PMACs(25). In one of the SAXS profiles the minima of the shape factor are marked by a dark triangle and the structure peak is marked by a single arrow. Successive profiles have been shifted vertically for clarity.

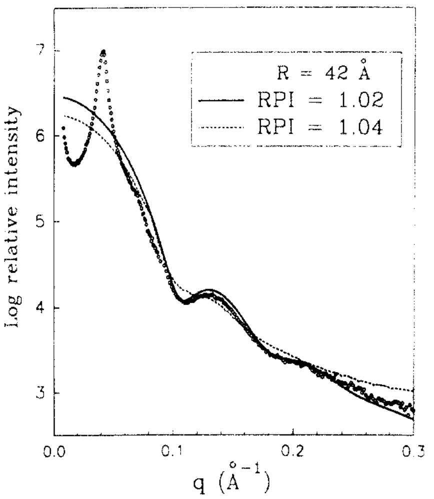

Figure 8. Typical fit of the shape factor peak for PS(170)-*b*-PMACs(25) with an ICPI of 2.1. The calculated shape factor curve for polydisperse spheres with a radius of 42 Å and an RPI of 1.02 is shown as a solid line, while the dashed line represents one with an RPI of 1.04.

the binary samples, while they are observed only in the samples of an ICPI up to 2.6 for the multicomponent blends. Figure 6 shows the SAXS intensity profiles for the PS-*b*-P4VPMeI samples prepared by method 3 for the multicomponent and the binary mixtures. The scattering patterns of the samples prepared by M3 are similar to those prepared by M2; however, the M3 binary samples show weak intensities for the shape factor peaks. It should be repeated here that the SAXS profiles of the "parent" block ionomers presented in Figure 6 were obtained on samples which were cast from DMF. It had been pointed out before[8] that there was no difference in peak positions and domain sizes between diblock ionomers (of low polydispersity) cast from DMF or THF. A *q* value of the first peak of the "parent" block lower than those of the blends seen in the binary blends is attributed to experimental artifact.

The SAXS profiles of the PS-*b*-PMACs system are shown in Figure 7. A sharp and symmetric peak accompanied by a shoulder is observed. For all samples, a broad and well-defined shape factor peak is present. A second shape factor peak could be identified for the sample with an ICPI of 1.1; however, this peak decreases for samples with ICPI values above 2.0. In all systems, the first two peaks or shoulders appeared in the range of relative angular positions of 1:1.6 to 1:1.9. The structure of these systems will be discussed more extensively in section 3.

Table 3. Relevant Parameters Obtained from Space-Filling Calculations for the PS-*b*-P4VPMeI Samples

	d' (Å)			N^b			S/N^c		
ICPI	M1[a]	M2[a]	M3[a]	M1[a]	M2[a]	Me[a]	M1[a]	M2[a]	M3[a]
				PS(470)-*b*-P4VPMeI(17)					
1.14	96	103	103	70	88	88	310	290	290
1.6	103	110	105	88	105	90	290	270	290
2.1	103	120	110	88	145	110	290	250	270
2.6	99	140	135	78	200	190	300	220	220
3.3	102	135	135	100	190	190	295	220	220
3.6	112	170	150	111	390	265	270	175	200
				PS(470)-*b*-P4VPMeI(26)					
1.1	85	105	118	71	133	188	400	330	300
1.5	91	107	90	85	142	85	380	320	390
1.7		113	100		167	110		310	360
2.0	91	122	105	85	210	120	380	290	340

[a] Assuming a sc lattice. [b] Number of chains per domain. [c] (Surface area)/(no. of chains).

3. Shape Factor Fit. The shallow minimum in the shape factor peak is a result of the polydispersity of sphere sizes. The polydispersity in the ionic microdomain sizes can be estimated by fitting the scattering profile of the shape factor peaks using the form factor for spheres with a Gaussian polydispersity. A detailed description of the fitting procedure[24] is published elsewhere and thus will not be repeated here. From the results of the fit, the radius of the ionic microdomains and the radius polydispersity index (RPI) were obtained. Typical fitting results are presented in Figure 8 for the diblock PS(170)-*b*-PMACs(25) of ICPI of 2.1, which give a radius of 42 Å and an RPI of 1.02. A shape factor for spheres with an RPI of 1.04 is also included in the figure. It can be seen that the minimum of the shape factor is smeared out considerably for spheres with high polydispersity. Note that the fitting of shape factor features was carried out for those samples in which a clear shape factor peak was observed. The results are given in Table 2 along with the values of the radii calculated from the structure peaks using space-filling calculations for the 4-vinylpyridinium methyl iodide system; those of the methacrylate diblocks are presented in Table 3. In general, the RPI values are small, ca. 1.03–1.05.

4. Variation of Radii of the Microdomains with ICPI. (i) PS-*b*-P4VPMeI Samples. Figure 9 represents the radii of the spherical domains as a function of ICPI for the PS-*b*-P4VPMeI multicomponent blends prepared by methods 1, 2, and 3. As mentioned in section 2, most of the radii values reported are obtained from shape factor features. For samples in which a shape factor is not observed, the R_{sc} values from space-filling calculations are reported. It can be seen from Table 2 that the sc lattice

Table 2. Values of the Radii of the Ionic Microdomains for the PS-*b*-P4VPMeI Samples

	R_{sc} (Å)[a]			R_{bcc} (Å)[a]			R_{fcc} (Å)[a]			R_{hcp} (Å)[a]			R_{shape} (Å)[b]			RPI[b]		
ICPI	M1	M2	M3	M1	M2	M3	M1	M2	M3	M1	M2	M3	M1	M2	M3	M1	M2	M3
								PS(470)-*b*-P4VPMeI(17)										
1.14	42	45	45	47	50	50	46	49	49	37	39	39	**42**	**44**	**44**	1.04	1.04	1.04
1.6	45	48	45	50	54	50	49	52	49	39	42	39		**48**	**46**		1.04	1.04
2.1	45	53	49	50	60	55	49	58	53	39	47	43	**47**	**53**	**50**	1.04	1.04	1.04
2.6	43	59	59	49	66	66	47	64	64	38	35	51	**45**	**57**		1.04	1.04	
3.3	44	59	59	50	66	66	48	64	64	39	35	51	**47**	**59**		1.06	1.04	
3.6	49	74	65	55	83	73	53	81	71	43	44	57		**74**			1.05	1.04
								PS(470)-*b*-P4VPMeI(26)										
1.1	48	60	67	54	67	75	53	65	73	42	52	58	**40**	**48**	**48**	1.03	1.04	1.04
1.5	51	61	51	58	68	58	56	66	58	45	53	45		**56**	**52**		1.04	1.05
1.7		64	55		72	62		70	62		56	49		**58**			1.03	
2.0	51	70	58	58	78	65	56	76	65	45	61	51		**60**			1.04	

[a] Values obtained from the structure peaks using space-filling calculations assuming different lattices. [b] Radius polydispersity index (RPI) values obtained from fitting the shape factor peaks using eq 1 in the text.

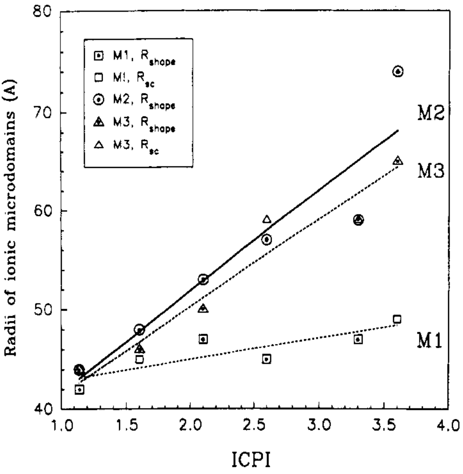

Figure 9. Radii of spherical ionic microdomains as a function of the ionic chain polydispersity index for the multicomponent blends of the poly(4-vinylpyridinium methyl iodide) samples prepared by methods 1, 2, and 3. The dotted symbols are values obtained from shape factor features. The hollow symbols are R_{sc} values (see text). The lines are linear regression lines through the data points.

gives values which compare best with those obtained from the shape factor features, when available. As noted earlier, this does not imply that these are the observed lattices for the system.

In Figure 9, there is a linear relationship between ICPI and *R* for the blends of PS-*b*-P4VPMeI copolymers prepared by methods 2 and 3. By contrast, PS-*b*-P4VPMeI samples prepared by method 1 show no variation between ICPI and *R*. Clearly, there is a strong dependence of the observed trends on the method of sample preparation. To explain this observation, one has to look at the detailed sample preparation methods, as discussed below.

Generally, when the solvent is evaporated, the solution becomes concentrated and eventually phase separation takes place. The surface energy between the ionic and the nonionic phase is very high, which suggests that the system will tend to maximize the size of the spheres to minimize the total surface area between the phases. This proceeds until the entropy cost of stretching the ionic chains is balanced by the surface energy gained through an increase in the radius of the spheres. Thus, the most favorable conformation in terms of energy minimization is for the longest chains to extend as much as possible, fixing the diameter of the spherical domain, while the shorter chains fill the space closer to the outer circumference. To achieve this conformation, the system should be at its thermodynamic equilibrium. The closer the system is to the thermodynamic equilibrium, the bigger are the sizes of the microdomains, up to the equilibrium values.

In method 2, the PS-*b*-P4VPMeI samples were cast from DMF, which is a good solvent for both blocks. Under these conditions, i.e., at high dilution, the copolymer chains do not aggregate yet.[25] As the solvent evaporates, the chains can rearrange during the phase separation process and thus attain the most favorable configuration in terms of energy minimization; i.e., the spherical domains are at their maximum size. In method 3, the PS-*b*-P4VP copolymers were mixed in THF before quaternization. Even though THF is a good solvent for the unquaternized PS-*b*-P4VP diblocks, it is a nonsolvent for the quaternized polymers. As a result, the polymers form micelles as they are being quaternized. However, the quaternization takes place over a long period of time (usually 4–5 h), which might give the P4VPMeI blocks some time to rearrange. It is also observed that the core radii of the blends prepared in THF are smaller than those prepared in DMF. It is suggested that the phase separation step of the PS-*b*-P4VPMeI diblocks in DMF occurs closer to thermodynamic equilibrium than in THF.

In method 1, the PS-*b*-P4VPMeI copolymers were mixed in DMF, where they are also single chains. When toluene, which is a nonsolvent for the P4VPMeI blocks, is added to the solutions, the P4VPMeI blocks phase separate into microdomains and the copolymers form micelle-like aggregates. Since the cmc of the PS-*b*-P4VPMeI copolymers in toluene is low (ca. 10^{-5} M[26]), the phase separation takes place even at a low toluene content. Further addition of toluene increases the selectivity of the solution. It seems reasonable to think that, once the micelles are formed, there is little exchange of the ionic chains between one microdomain and another. Thus, the sizes of the spherical microdomains are fixed at the time of localization. It is believed that the materials are trapped in a nonequilibrium state. This also results in a smaller domain size. It should be noted that, for the samples prepared by method 1, core sizes smaller than those prepared by methods 2 or 3 are observed.

To see if dual morphology is present, i.e., if the short and the long ionic segments separate from one another to form their own morphology, we looked at the binary blends in which the very short P4VPMeI blocks (17 units) were mixed with a variety of longer P4VPMeI blocks (52, 71, and 94 units). In this case, the number-average molecular weight of the ionic block is kept at 26 units. The same relation between the radii of the microdomains and the ICPI is observed for the binary blends as for the multicomponent blends of the PS-*b*-P4VPMeI materials prepared by methods 1, 2, and 3. From the SAXS profiles (Figures 4–6), it can be seen that there is no difference in scattering patterns between mixed samples of 17 and 52, those of 17 and 71, and those of 17 and 94; furthermore, shape factor peaks for spheres are seen in all cases. The TEM micrograph (Figure 3) shows only spherical ionic domains. It is concluded that dual morphology does not exist in the systems studied.

The binary blends also demonstrate the fact that it is the long chains which determine the radius of the microdomains. For example, the radius of the binary blend prepared by method 2 of PS(473)-*b*-P4VPMeI(26) of ICPI of 1.5, which is composed of ionic chains of 52 and 17 units is 56 Å, while that of the unmixed PS(473)-*b*-P4VPMeI-(52) of ICPI of 1.11 is 55 Å, identical to that of the blend.

(ii) PS-*b*-PMACs. In Figure 7, it is observed that, for the PS-*b*-PMACs system, the structure peaks of all the samples with different ICPI values are in the same position. Since the volume fractions of the ionic segments are constant in these samples, the values of the radii, as obtained from space-filling calculations, are all the same (Table 4). Thus, the radii of the microdomains stay constant as the ICPIs change. To understand the observation, one has to look at the process of sample preparation.

The PS-*b*-PMAA copolymers are soluble in THF when they are in the acid form, but when they are neutralized, the ionomers form micelles in solution. It is known that the methacrylic acid diblocks in THF form micelles after the addition of the first few milliliters of methanolic cesium hydroxide.[21] Micellization traps the ionic segments, and as the solution becomes more concentrated, the system is no longer at equilibrium. This process is similar to that of the PS-*b*-P4VPMeI samples prepared by method 1, where similar results are obtained. It is interesting to note that the nonequilibrium state, which is operative in

Table 4. Results Obtained for the PS(170)-*b*-PMACs(25) Samples

ICPI	R_{sc} (Å)[a]	R_{bcc} (Å)[a]	R_{fcc} (Å)[a]	R_{hcp} (Å)[a]	R_{shape} (Å)[b]	RPI[b]	d' (Å)[c]	N[c]	S/N[c]
1.1	50	56	55	44	52	1.02	82	155	210
1.6	51	57	55	44	44	1.03	82	155	210
2.1	50	56	55	44	42	1.03	82	155	210
2.6	55	62	60	48	44	1.03	86	175	210
3.1	54	61	59	47	44	1.03	86	175	210

[a] Values obtained from the structure peaks using space-filling calculations assuming different lattices. [b] Values obtained from the fit of the shape factor peaks using eq 1 in the text. [c] Values calculated by space-filling calculations assuming an hcp lattice. N = number of chains per domains. S/N = (surface area)/(no. of chains).

systems of PS-*b*-PMAA and PS-*b*-P4VPMeI prepared by method 1, is produced by two different paths. While in the P4VPMeI system it is the result of the addition of a nonsolvent into the single-chain polymer solution, for the methacrylate samples it is a consequence of the neutralization condition of the acid copolymers.

It is also observed from Figure 7 that the shape factor peaks of the blends are at a higher q value (smaller radius) than those in the unmixed sample. For the unmixed copolymer, the R_{sc} value is best compared to that calculated from the shape factor peaks. However, for the blends, the R_{hcp} (spheres on a hexagonal lattice) values are closest to the values calculated from the shape factor peaks. It is possible that the polydispersity in the PS-*b*-PMACs system causes the system to change the packing.

Finally, the results concerning the sizes of the microdomains confirm the finding that the ionic chains are highly extended in their domains, as was observed in a previous study from this laboratory[4,8] and also in the study by Vankateshwaran *et al.*[6] The planar zigzag chain length of a 25 unit chain of PMAA is 62 Å, and the experimental average value obtained is 50 Å. The experimental values of the radii of the spherical domains in the vinylpyridinium samples are in the range 45–74 Å, while the planar zigzag chain length of a 17 unit chain of P4VPMeI is 42 Å.

5. Discussion of Other Parameters (N,S/N,d'). From the values of the radii of the microdomains, the Bragg distances, and the volume fraction of the blocks, it is possible to calculate the surface to surface distances between spheres (d'), the aggregation number (N), and the surface area per chain (S/N), which is the total surface area divided by the aggregation number. For the sake of completeness, these results are listed in Table 3 for the PS-*b*-P4VPMeI system and Table 4 for the PS-*b*-PMACs series.

It is observed that d' and N are unchanged for the methacrylate series and for the vinylpyridinium samples prepared by method 1; by contrast, they increase with the ICPIs for the vinylpyridinium samples prepared by methods 2 and 3. Thus, the relation between d' or N with ICPI is the same as that found for the radii. Finally, the decrease of the value of S/N in the PS–P4VPMeI diblocks prepared by methods 2 and 3, as seen in Table 3, is a consequence of the increasing values of N. For these samples, it can be concluded that the higher the polydispersity, the more compact is the packing of the spheres.

Conclusions

The present study explores the effect of the ionic chain polydispersity on the morphology of the spherical ionic microdomains. Samples are prepared by mixing diblock ionomers of constant polystyrene chain lengths and different ionic block lengths. The ratio of mixing is determined so that in a set of samples the number-average molecular weights stay constant but that a wide range of polydispersity in the ionic blocks is obtained. Multicomponent and binary blends are prepared by three different methods. In the first method, they are prepared from solutions in which a nonequilibrium state exists. This is achieved either by adding a nonsolvent to the single-chain polymer solution of the 4-vinylpyridinium methyl iodide samples or by neutralizing the methacrylic acid copolymers in a selective solvent. In the second method, the 4-vinylpyridinium methyl iodide samples are mixed and cast from DMF, which is a good solvent for both blocks. In the third method, the 4-vinylpyridine diblocks are mixed prior to quanternization; they are subsequently quaternized and cast from THF.

Transmission electron micrographs of the blends show spherical ionic microdomains. No dual morphology is observed even for the binary blends in which only two but very different ionic block lengths are mixed together.

It is concluded that the effect of ionic chain polydispersity on the sizes of the ionic microdomains depends on the method of sample preparation. When the samples are prepared close to thermodynamic equilibrium, e.g., cast from a good solvent for both blocks, the values of the radii of the ionic domains vary linearly with the ionic chain polydispersity. This is seen for the polystyrene-*b*-poly(4-vinylpyridinium methyl iodide) samples prepared by methods 2 and 3. It is suggested that in these samples the longest chains are extended as much as possible and fix the radius of the microdomains, while the shorter chains take up the regions closer to the surface. However, if the samples are prepared under severe conditions such as those which lead to micellization of the copolymers, the polydispersity does not have any effect on the sizes of the domains. This is found for the polystyrene-*b*-poly(cesium methacrylate) diblocks and for the polystyrene-*b*-poly(4-vinylpyridinium methyl iodide) samples prepared by method 1.

Acknowledgment. D.N. is grateful to Le Fonds pour la Formation de Chercheurs et l'Aide à la Recherche (Quebec) for graduate scholarships. We thank Dr. A. Desjardins for the PS-*b*-PMAA samples.

References and Notes

(1) Selb, J.; Gallot, Y. In *Developments in Block Copolymers—2*; Goodman, I., Ed.; Elsevier Applied Science: London, 1985; Chapter 2.

(2) Isono, Y.; Tanisugi, H.; Endo, K.; Fujimoto, T.; Hasegawa, H.; Hashimoto, T.; Kawai, H. *Macromolecules* **1983**, *16*, 5.

(3) Gauthier, S.; Eisenberg, A. *Macromolecules* **1987**, *20*, 760.

(4) Gouin, J. P.; Williams, C. E.; Eisenberg, A. *Macromolecules* **1989**, *22*, 4573.

(5) Gouin, J. P.; Williams, C. E.; Eisenberg, A. *Macromolecules* **1992**, *25*, 1368.

(6) Venkateshwaran, L. N.; York, G. A.; DePorter, C. D.; Long, T. E.; McGrath, J. E.; Wilkes, G. L. *Polymer* **1992**, *33* (11), 2277.

(7) Desjardins, A.; Eisenberg, A. *Plastics, Rubber and Composites Processing and Applications* **1992**, *18*, 161.

(8) Gouin, J. P.; Bosse, F.; Nguyen, D.; Williams, C. E.; Eisenberg, A. *Macromolecules* **1993**, *26*, 7250.

(9) Lu, X.; Steckle, W. P.; Weiss, R. A. *Macromolecules* **1993**, *26*, 6525.

(10) Eisenberg, A. *Macromolecules* **1970**, *3*, 147. Eisenberg, A.; King, M. In *Ion-Containing Polymers*; Academic: New York, 1977.

(11) Nyrkova, I. A.; Khokhlov, A. R.; Doi, M. *Macromolecules* **1993**, *26*, 3601.

(12) Mori, K.; Tanaka, H.; Hasegawa, H.; Hashimoto, T. *Polymer* **1989**, *30*, 1389.

(13) Zhulina, E. B.; Birshtein, T. M. *Polymer* **1991**, *32*, 1299.

(14) Desjardins, A.; Eisenberg, A. *Macromolecules* **1991**, *24*, 5779.

(15) Long, T. E.; Allen, R. D.; McGrath, J. E. In *Chemical Reactions on Polymers*; Benham, J. L., Kinstel, J. F., Eds.; ACS Symposium Series 364; American Chemical Society: Washington, DC, 1988; Chapter 19.

(16) Gauthier, S.; Duchesne, D.; Eisenberg, A. *Macromolecules* **1987**, *20*, 753.

(17) Bates, F. S.; Hartney, M. A. *Macromolecules* **1985**, *18*, 2478.

(18) Leibler, L.; Benoit, H. *Polymer* **1981**, *22*, 195.

(19) Elias, H. G. *Macromolecules: Synthesis and Materials*; Plenum Press: New York and London, 1977.

(20) Storey, R. F.; George, S. E. *Polym. Mater. Sci. Eng.* **1988**, *58*, 985.

(21) Dubuisson, J. M.; Dauvergne, J. M.; Depautex, C.; Vachette, P.; Williams, C. E. *Nucl. Instrum. Methods* **1986**, *A246*, 636.

(22) Glatter, O.; Kratky, O. In *Small Angle X-Ray Scattering*; Academic Press: New York, 1982.

(23) Williams, C. E. In *Neutron, X-Ray and Light Scattering: Introduction to an Investigative Tool for Colloidal and Polymeric Systems*; Lindner, P., Zemb, Th., Eds.; North-Holland: Amsterdam, 1991; p 101.

(24) The volumes of the polymer units were calculated with the following densities: 1.05 g/mL for PS, 1.6 g/mL for P4VPMeI, and 1.7 g/mL for PMACs, as determined by pycnometry.

(25) Nguyen, D.; Williams, C. E.; Eisenberg, A. *Macromolecules*, submitted.

(26) Gauthier, S. Ph.D. Thesis Dissertation, McGill University, 1985.

(27) Khougaz, K.; Zhong, X. F.; Eisenberg, A., manuscript in preparation.